

Molecular simulation study of alkyl monolayers on the Si(111) surface

Shi-Ling Yuan,^{*a} Zheng-Ting Cai^a and Yuan-Sheng Jiang^{ab}

^a Institute of Theoretical Chemistry, Shandong University, Jinan 250100, P. R. China.
E-mail: shilingyuan@sdu.edu.cn; Fax: +86 531 856 4464; Tel: +86 531 856 4750

^b Institute of Theoretical and Computational Chemistry, Nanjing University,
Nanjing 210093, P. R. China

Received (in Montpellier, France) 14th August 2002, Accepted 18th November 2002

First published as an Advance Article on the web 24th January 2003

The structure of eight-carbon monolayers on the H-terminated Si(111) surface was investigated by a molecular simulation method. Molecular mechanics calculations showed that the best substitution percentages on the Si(111) surface were 50% for octene or octyne-derived monolayers and 40% for the styrene or phenylacetylene-derived monolayers. These values are in good agreement with the experimental results. After a two-dimensional cell containing alkyl chains and four layers of Si atoms was constructed, the densely packed and well-ordered monolayer on the Si(111) surface can be shown at the molecular level. At the same time, the thickness of the monolayers and the tilt angle of the alkyl chain were also calculated. Additionally, the theoretical calculations showed that the C≡C bond of the alkyne only reacts once with the H-terminated Si(111) surface, that is only one Si–C bond per organic molecule is formed on the Si(111) surface, which verifies the experimental results. It is thus shown that molecular simulation can provide otherwise inaccessible microscopic information at the molecular level, and may be considered as a useful adjunct to experiments.

1. Introduction

The preparation of monolayers on silicon surfaces is of growing interest for potential applications in biosensor or semiconductor technology. Alkyl-modified Si(111) surfaces can be obtained using the thermal, catalyzed, or photochemical reaction of hydrogen-terminated silicon with alkenes,^{1–4} Grignard reagents,^{5–8} aldehydes,⁹ or by the electrochemical reduction of aryldiazonium ions.¹⁰ The properties of the monolayer on Si(111) surfaces have been studied by a variety of experimental methods such as X-ray photoelectron spectroscopy (XPS),^{11–14} Fourier transform infrared absorption spectroscopy (FTIR),^{15,16} scanning electron microscopy (SEM),⁴ ellipsometry,^{8,17} Auger electron spectroscopy (AES),¹⁸ and scanning tunneling microscopy (STM).^{19–21} These experimental results can help us to understand the densely packed, well-ordered monolayer on Si(111) surfaces.

Besides the experiments above, some theoretical calculations have also been performed to investigate the structures on small Si surfaces using quantum mechanics methods.^{22–24} These calculations can give the microscopic properties of the organic monolayer at the atomic level, such as the interaction energy or bond length between two atoms on the Si(111) surface. However, it is difficult to investigate the structure of a big monolayer system containing several hundred atoms in a quantum mechanics calculation. Recently, several molecular simulation methods were developed to investigate the geometry of alkyl monolayers on Si(111) surfaces,^{25,26} and some interesting results were obtained. For example, it was found that the substitution percentage of C₁₈ alkyl monolayers, that is the ratio between the number of H-atoms and the number of alkyl chains on the first layer of the Si(111) surface, was approximately 50%, in good correlation with the available experiment data. Zhang *et al.* also discussed the detailed packing structures of C₁₈ alkyl monolayers and the temperature effect on the properties of alkyl monolayers.²⁶ These molecular mechanics

calculations can offer some microscopic information on the monolayer at the molecular level.

In 2000, Cicero *et al.* reported the photoreactivity of H–Si(111) with dioxygen and terminally unsaturated hydrocarbons (1-octene, 1-octyne, styrene and phenylacetylene) and experimentally determined the monolayer thickness and substitution percentage on the Si(111) surface,²⁷ but theoretical investigations on the microscopic structure properties corresponding to Cicero's work have not been reported. In this paper, we will study the molecular packing structures, substitution percentage and packing energies of monolayers of eight-carbon adsorbates using the molecular mechanics method.

2. Methods

All molecular mechanics calculations were performed using the MSI program Cerius². The Minimizer module was used to calculate the energies of different simulation systems. The structures were optimized using the universal force field²⁸ (UFF) and the “Smart Minimizer” method with “high-convergence” criteria.²⁵ At the same time, in order to compare with some of the simulation conclusions, another force field, COMPASS,^{29,30} was also used. However, in the case of COMPASS, the “ignore undefined terms” program option was selected, as this force field does not contain inversion parameters for the Si atoms with a dangling bond at the bottom of the Si crystal (please see Fig. 1). This reduction of the system does not affect the optimization of the monolayer.

Firstly, a crystal structure of silicon containing 8 Si atoms was constructed; then the Si(111) surface was cleaved from the crystal lattice, and four layers of Si atoms were selected on the surface; an alkyl chain was linked to the Si atom in the first layer. Finally, a 3.840 Å × 3.840 Å × 28.000 Å small unit cell for molecular mechanics studies was built, which consists of one alkyl chain perpendicular to the Si(111) surface and four Si atoms that represent the atoms in the four-layer

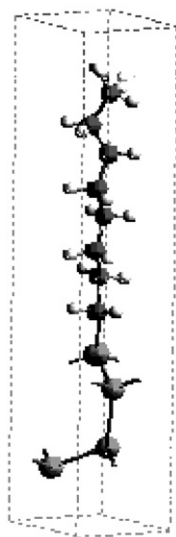


Fig. 1 Structure of the repeating unit (including one alkyl chain perpendicular to the Si surface and four Si atoms that represent the atoms in the first four layers of the Si surface).

structures of the Si(111) crystal (Fig. 1). The unit cell can be repeated in the x and y directions to generate one-dimensional (for example: 1×2 , 1×3) or two-dimensional (for example: 2×4 , 4×8) simulation cells.

After the input geometries of different substitution patterns have been constructed in the simulated cells, the structures of the one-dimensional or two-dimensional simulated systems are optimized, and the energy (E) of the systems can be calculated by molecular mechanics. When all the alkyl chains in the simulated cells are substituted by H atoms, the energy (E_0) of the Si atoms in the systems can be calculated. Thus, the energy (E_1) per alkyl chain is obtained *via* the following formula:

$$E_1 = \frac{E - E_0}{N} \quad (1)$$

where N represents the number of alkyl chains in the simulated system.

3 Results and discussions

3.1 Molecular substitution percentage

Alkyl monolayers on Si surfaces are obtained by the following experimental steps: firstly, native oxides from Si(111) are removed by an aqueous NH_4F etch and a hydrogen-terminated silicon(111) surface is obtained; then, the hydrogen atoms on the Si surface are substituted with unsaturated hydrocarbons *via* an alkylation procedure. Thus, the hydrophilic Si surface can be converted into a hydrophobic surface. In this alkylation procedure, different substitution percentages on the Si surface are obtained when different experimental technologies are used. For example, Terry *et al.* found that the pentane molecular substitution percentage was 60%;³¹ but Effenberger *et al.* indicated that the octadecane molecular substitution percentage was 97%.⁹ The difference obtained in the experiments are mainly due to the use of different techniques, not the number of carbon atoms in the alkyl chain. A molecular mechanics simulation²⁵ has shown that octadecane molecular substitution is about 50%. This result is in good agreement with the Linford's experiment.¹ In this paper, we discuss the same problem for monolayers of eight-carbon adsorbates.

Different one-dimensional simulation cells including 1×1 , 1×2 , 1×3 and 1×4 simulation systems were designed through the unit cell, which are repeated in the x direction. These simulation cells, in which some alkyl chains are

substituted by hydrogen atoms, represent different molecular substitution percentages from 20% to 100%. Fig. 2 shows the molecular energy per alkyl chain as a function of the molecular substitution percentages. Obviously, as shown in Fig. 2(a) and (b), the lowest energy per molecule for the octene- or octyne-derived monolayers was found at a substitution percentage of 50%, which implies that the best substitution percentage is 50%; for the same reason, the best percentage is 40% for the styrene- or phenylacetylene-derived monolayers. In order to verify the conclusion above, the COMPASS force field was used to calculate the energy per alkyl chain for octene- or octyne-derived monolayers. In Fig. 2(c), we can conclude that the energy at 50% substitution is still the lowest. Because the UFF and COMPASS force fields give the same results, both can be used to study the substitution percentage, pattern and the other parameters on Si(111) surface. However, the COMPASS requires expensive CPU time for the big simulation

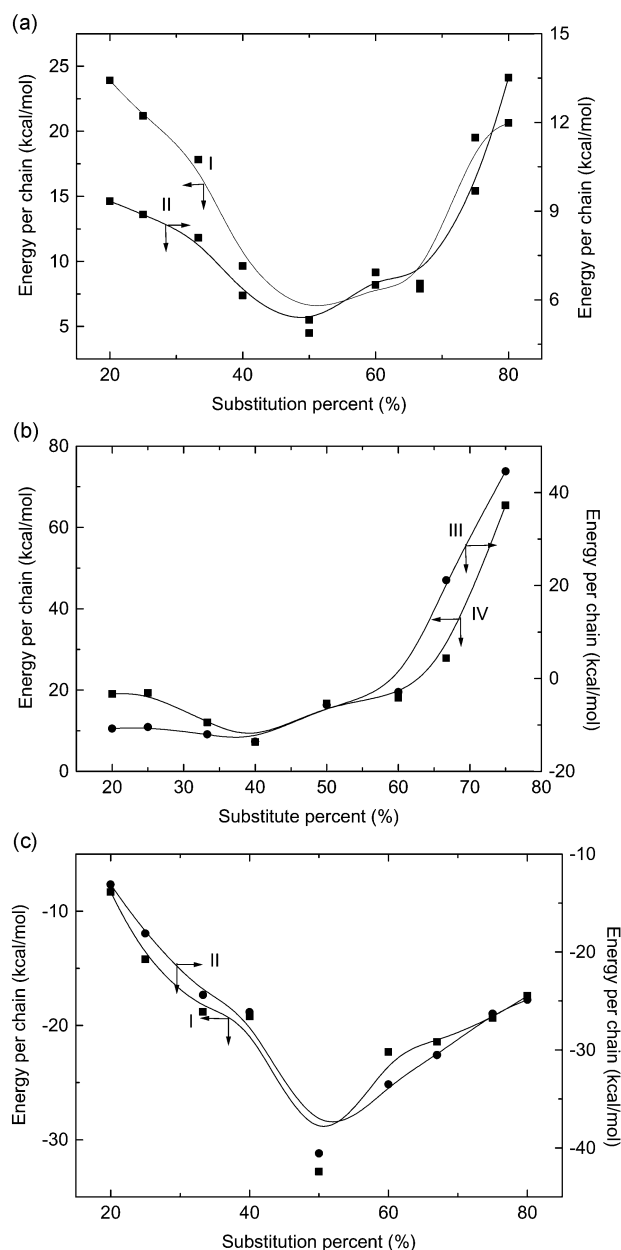


Fig. 2 The energy per alkyl chain *vs.* substitution percentage. (a) UFF-calculated energy per alkyl chain for octene- (I) or octyne-derived (II) monolayer systems; (b) UFF-calculated energy for styrene- (III) or phenylacetylene-derived (IV) systems; and (c) COMPASS-calculated energy for octene- or octyne-derived monolayer systems.

Table 1 Surface composition

Adsorbate	% Substitution ^a	Thickness ^a / Å	% Substitution ^b	Thickness ^b / Å
Octene	44	9	50	11
Octyne	45	10	50	11
Styrene	34	10	40	8
Phenylacetylene	36	10	40	8

^a Experimental results.²⁷ Errors in substitution percentage are $\pm 3\%$ and in thickness are ± 2 Å. ^b Molecular mechanics calculated results.

system. Therefore, only the UFF force field will be used in the following calculations.

Comparing Fig. 2(a) with Fig. 2(c), one can see that the energies per alkyl chain are different at the same substitution percentage of octene- or octyne-derived monolayers, and the UFF-calculated energy is positive, while the COMPASS-calculated energy is negative. It is easy to understand that the energy values could be different using different force field methods although the same simulation system was selected, and the energy should be only a relative value, not the absolute value. So we concentrate on the variation in the energy per chain with the increase of substitution percentage and make comparisons within the same series in this paper.

In Fig. 2, it is shown that the substitution percentage of octene- or octyne-derived monolayers is bigger than that of the styrene- or phenylacetylene-derived monolayers. The energy per chain of the octene- or octyne-derived monolayer at 50% [Fig. 2(a)] is obviously the lowest compared with the energy at other substitution percentages from 20% to 80%. In the other words, curves I and II [in Fig. 2(a)] have an obvious energy trap around 50% substitution. In contrast, curves III and IV [in Fig. 2(b)] relative to the styrene- or phenylacetylene-derived monolayers vary little from 20% to 60%. At small substitution percentages, the disordered and long alkyl chains of the octene- or octyne-derived monolayers occupy a larger space than the disordered and short alkyl chains of the styrene- or phenylacetylene-derived monolayers. The difference between the curves in Fig. 2(a) and (b) is mainly due to the steric effect of hydrocarbon chain. For octene- or octyne-derived monolayer, maybe 50% substitution can be easily obtained in experiments, while for styrene- or phenylacetylene-derived monolayers, 30–40% substitution has a similar possibility, that is the percentage obtained in the experiment maybe has an uncertainty error.

The thickness and substitution percentages for H-modified Si(111) surfaces from molecular simulation and experiments are given as pairs of data in Table 1. These data indicate that the calculated substitution percentages are in good agreement with the experimental results. It is difficult to draw the molecular structure on a Si(111) surface at 52% or 38% substitution percentage when designing the simulated cells, so the final simulation results may have small errors, and the calculated results can only qualitatively explain some experimental phenomena.

3.2 Molecular substitution pattern for octene- or octyne-derived monolayers

In the discussion above, the best substitution percentage of octene- or octyne-derived monolayers on a Si(111) surface is 50%, which is similar to the experiment results of $45 \pm 3\%$.²⁷ Because it is difficult to design structures at 48% or 42% substitution for the calculations on Si(111) surfaces,²⁷ a substitution percentage of 50% is a very convenient choice, and will be used below. Fig. 3 shows some simulation cells with different substitution patterns on the Si(111) surface. The designed simulation cells have different substitution patterns a–k, which are in the (2×2) , (2×3) and (2×4) simulation cells,

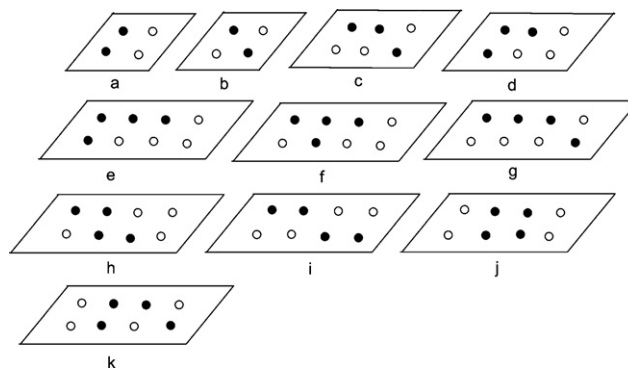


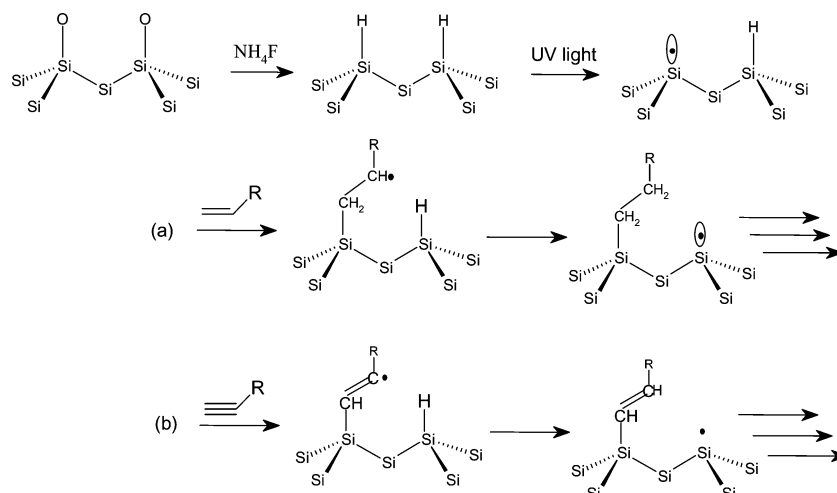
Fig. 3 Simulation cells of different substitution patterns at 50% substitution for octene- and octyne-derived monolayers. These cells are considered as (2×2) , (2×3) and (2×4) simulation cells, respectively. The black dots represent alkyl chains and the white dots represent hydrogen atoms on the first Si surface.

respectively. The energy per chain for these substitution patterns as calculated by molecular mechanics is listed in Table 2. As noted above, the energies should be viewed as relative energies, which can only be used to compare among different substitution patterns for series of monolayers.

As shown in Table 2, the energy per alkyl chain of pattern i for octene- or octyne-derived monolayers is the lowest. The energies of patterns g and k for the octene-derived monolayer, and of g for the octyne-derived monolayer are relatively low. So one conclusion is that patterns i and g are stable structures in contrast to the other patterns for octene- or octyne-derived monolayers. Alkyl chains in the substitution patterns g and k are packed very closely and molecular interactions twist the chains, which results in disordered packing structures in our simulation. Therefore, in the following, substitution pattern i for the C_8 alkyl chain is used for further study on how molecular orientation affects the structures of octene- or octyne-derived monolayers on a Si(111) surface. In previous studies,^{25,26} pattern i for the C_{18} alkyl chain was also selected for more in-depth discussions. Table 2 also shows that the loose patterns containing at least two nearby alkyl chains have relatively low energies, such as patterns d, e, g, i and k. This means that the interaction between alkyl chains is very important for the loose substitution patterns. However, the energies of the concentrated substitution patterns, such as f and j, are relatively high. The energy of substitution pattern j containing four alkyl chains in a square configuration is the highest. This indicates that not only van der Waals interactions among alkyl chains on the Si(111) surface but also the steric effects of alkyl chains are important to the structures of alkyl monolayers.

Table 2 The energies per alkyl chain on the Si surface for different substitution patterns at 50% substitution

Substitution pattern	Simulation cell	Energy per chain/kcal mol ⁻¹	
		Octene-derived	Octyne-derived
a	(2×2)	−4.828	−10.694
b	(2×2)	−2.568	−8.378
c	(2×3)	−1.948	−10.717
d	(2×3)	−3.412	−9.171
e	(2×4)	−3.667	−15.727
f	(2×4)	−1.546	−7.886
g	(2×4)	−10.329	−19.243
h	(2×4)	−2.783	−6.476
i	(2×4)	−12.301	−20.857
j	(2×4)	1.568	12.339
k	(2×4)	−11.643	−8.7409



Scheme 1 Photoinitiated free radical mechanism for the reaction of a Si surface containing native oxides with octene or octyne. Silicon surface dangling bonds are formed by UV light illumination. Reactions (a) and (b) show the normal alkylation procedure, *i.e.* a secondary carbon radical abstracts a neighboring hydrogen to produce a new surface dangling bond.

3.3 The explanation of substitution patterns of the octene-derived monolayer on a Si(111) surface

It is well-known that how an alkyl monolayer on a Si(111) surface is formed can be interpreted using a free radical mechanism under conditions of UV illumination.^{27,32} A terminal olefin molecule is first added to a silicon radical to form a covalent C–Si bond. A neighboring surface hydrogen atom is then abstracted by the resulting secondary carbon radical to regenerate a new silicon radical. This process can be repeated many times to yield many adsorbates per initiation event.²⁷ Scheme 1 shows the free radical mechanism for addition of a terminal octene or octyne to silicon radicals on a Si(111) surface containing native oxides.

The energy per alkyl chain of the different substitution patterns can be used to discuss the substitution process. As shown in Fig. 4, a platform of a (4 × 4) simulation cell can reflect the substitution process of the free radical mechanism on an

H-terminated Si surface. In the first layer of the silicon surface, four neighboring atoms form a rhombus with an obtuse angle of 120° (see Fig. 4), in which the lengths of the two diagonals are different, with the length of the short diagonal being equal to the side length of the rhombus. Therefore, a short distance is favorable to the formation of the secondary silicon free radical when only the steric effect is considered. So, the possibilities in which a hydrogen atom on the neighboring Si atom is abstracted by the carbon atom in the alkyl chain along the side of the rhombus should be equal to that along the short diagonal. The probability of producing another free radical along the long diagonal is lower than that along the short diagonal or the side of the rhombus. That is, the next-nearest Si atom is favored for the free radical substitution. Thus, a random H atom on a Si(111) surface abstracted by the terminal C atom in the alkyl chain has six possibilities, which are equally probably. In Fig. 4(A), the second substitution is selected to represent one of the probabilities.

The third alkyl substitution on the Si(111) surface has three possibilities [see Fig. 4(B), (C) and (J)]. But the distance between the hydrogen atom at the (iii, ii) site and the first alkyl substitution site (ii, i), is shorter than that between the first alkyl substitution site and the hydrogen atom site at (ii, iii) or (iii, iii). In addition, a short distance between the first and the third substitution site is unfavorable to alkylation due to steric repulsion effects. Thus, the calculated energy shows that the energy per alkyl chain of substitution pattern J is higher than that of patterns B or C (see Table 3). Thus, only two substitution probabilities, B and C, for the third abstracted hydrogen atom on the Si(111) surface are viable.

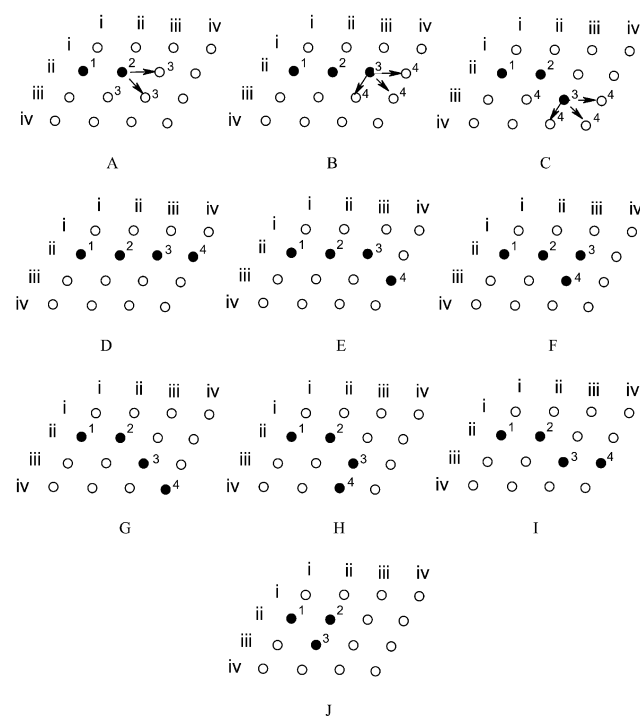


Fig. 4 Sketch map of the substitution process for an alkyl chain on the Si(111) surface.

Table 3 The energies per alkyl chain on the Si surface for sequential substitutions of the octene-derived monolayer

Substitution pattern	Energy per chain/kcal mol ⁻¹
A	–25.681
B	–30.168
C	–30.696
D	–10.507
E	–24.258
F	–24.120
G	–26.884
H	–27.092
I	–27.083
J	–29.461

For the substitution pattern B, there are also three possibilities for the fourth substitution sites when considering the short distance effect between the fourth and the first or the second alkyl chain, that is, substitution patterns D, E and F. Table 3 shows that the highest energy is found for a linear 4-alkyl pattern [Fig. 4(D)], which indicates that the probability of substitution pattern D is the lowest and this pattern unfavorable.

Similarly, for substitution pattern C, there are three possibilities for the fourth substitution site with the considerations above: G, H and I. As listed in Table 3, one can see that the energies of substitution patterns G, H and I are lower than those of substitution patterns D, E and F. This indicates that choice of the third substitution, B or C, can affect the fourth substitution site, and the substitution pattern C should be more favorable for radical substitution when only considering the energy per alkyl chain. The free radical mechanism can be summarized as follows: (1) the third site of free radical substitution should adopt the next-nearest rule and be far from the first substitution site due to steric effects; (2) patterns containing two or three nearby alkyl chains are favorable to sequential substitution; (3) the fourth substitution must change direction if the former ones are in-line on the Si(111) surface. From the discussion above, the substitution pattern i in Fig. 3 should have a high probability.

3.4 The effect of the number of alkyl chains in simulation cells

After pattern i of octene or octyne-derived monolayer had been selected, it was necessary to search for the size-appropriate simulation cell, in which the micro-structure and other information on the alkyl monolayer on the Si(111) surface can be obtained, the appropriate cell meaning one for which little CPU time is needed. In other words, we need not spend expensive CPU time on the big system, and our aim is to look for a small Si surface that reflects the properties of the big system. In our simulations, domain boundaries were used to restrict the simulation cell. This indicates that the alkyl chains at the boundaries and those in the center have the same environment. Thus, although the two-dimensional cells have limited spaces, theoretically speaking, the analysis for small simulation cells can represent the properties of big simulation systems. In the presence of boundary conditions, the (2×4) , (4×4) , (4×8) , (8×8) and (8×16) two-dimensional simulation cells, in which the numbers of alkyl chains range from 4 to 64, can be designed by repeating the (2×4) unit cell in the x and y dimensions. Fig. 5 shows the relationship between the number of alkyl chains in the simulation cells and the energy per alkyl chain or the tilt angle of the alkyl chain in these simulation

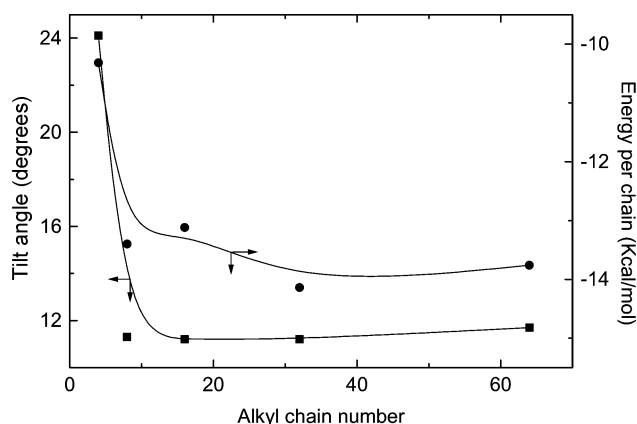


Fig. 5 Alkyl chain number in simulation cells versus energy per chain and the tilt angle of the alkyl chain.

systems. One can see that the energy per alkyl chain and tilt angle of octene-derived monolayers are invariable when the number of alkyl chains is equal to 32 or 64. Therefore, the (8×8) or (8×16) simulation cell can be used to study the structures of alkyl monolayers. For the other systems, such as octyne-, styrene or phenylacetylene-derived monolayers on a Si(111) surface, the values of the energy per chain and the tilt angle of the alkyl chain show that the (8×8) or (8×16) simulation cell can also be used to investigate the micro-structural properties on a Si surface *via* molecular mechanics calculations. So, in the following discussions, an (8×16) simulation cell will be selected.

3.5 Alkyl chain geometry of an octene-derived monolayer on a Si surface

Before optimization, the input geometry of the substitution pattern i in a (8×16) simulation cell contains 64 hydrogen atoms and 64 alkyl chains, which are perpendicular to the first layer of the Si(111) surface. After optimization using molecular mechanics, all the alkyl chains tilt towards the Si surface [Fig. 6(a)]. The tilt angle is around 10° and the calculated thickness is $10.8 \pm 0.2 \text{ \AA}$, in good agreement with the $9 \pm 2 \text{ \AA}$ reported in the literature (see Table 1).²⁷ In addition, an interesting phenomenon can be found in the optimized monolayer on the Si surface. The input geometry of the alkyl chains on the Si surface before optimization took on a “z-form” [top view shown in Fig. 6(b)]; however, the distribution of alkyl chain became uniform when the molecular mechanics optimization was performed [Fig. 6(c)]. This distribution is the result of steric effects and the interactions between alkyl chains. The ordered geometry of the alkyl monolayer is favorable to the macroscopic properties, some experiments have proven the existence of densely packed, well-ordered monolayer structures on the Si(111) surface.^{14,27} Molecular mechanics results can reproduce the steric structures of alkyl monolayers on Si(111) surface at the molecular level and support the experimental results.

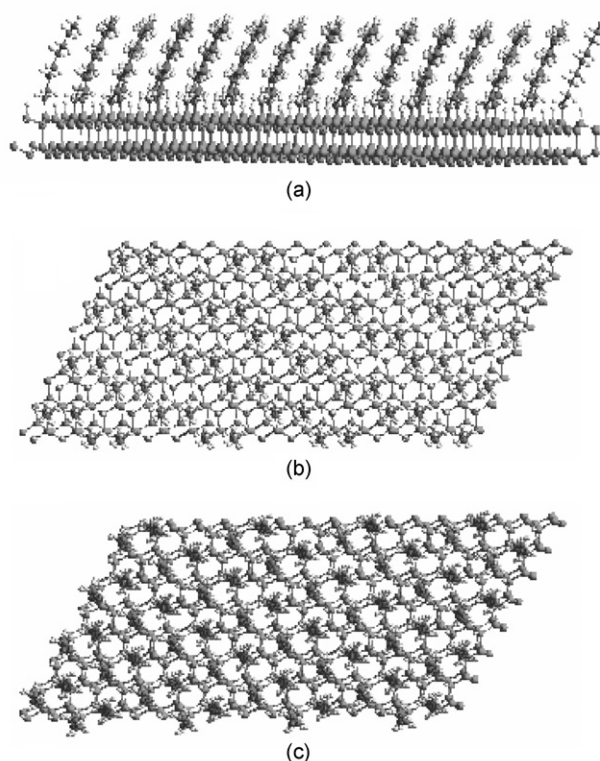
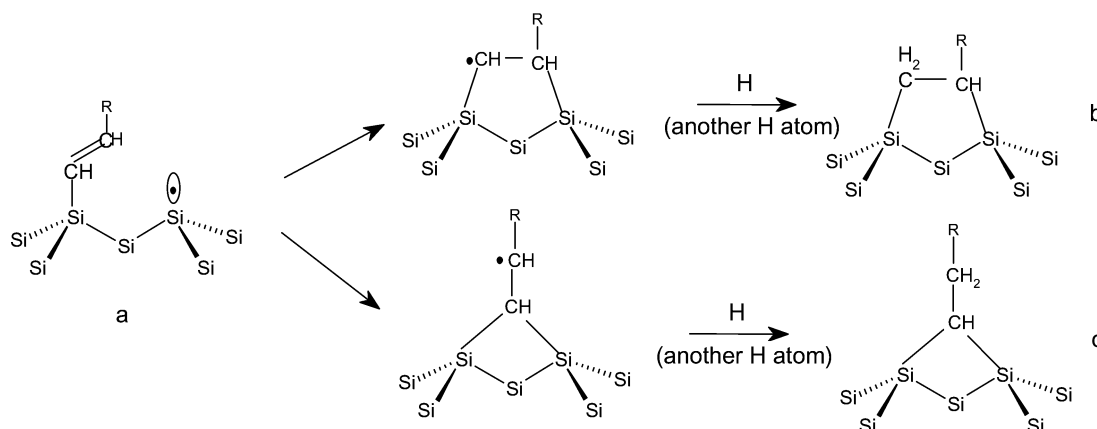


Fig. 6 Alkyl monolayer on a Si surface before and after optimization: (a) side view of the optimized geometry, (b) and (c) top view of the input and optimized geometries.



Scheme 2 Mechanism of the reaction of 1-alkyne with an H-terminated Si(111) surface, depicting the possible formation of 2 Si-C bonds per molecule.

3.6 The possible formation of alkyne-derived monolayers on Si surfaces

Some literature reports have shown that the C≡C bond of alkyne can react either once^{1,27,32,33} or twice³⁴ with a surface Si-H group, depending on the reaction conditions. On a Si(100) surface or porous silicon, the thermal or catalyzed reaction of alkyne has been reported to give two Si-C bonds per molecule,³⁴ meaning that C=C bonds are not found in the alkyne-derived monolayers. However, on a Si(111) surface, only one Si-C bond per molecule is formed using thermal or photochemical reactions.^{1,27} Cicero *et al.* observed a weak C=C bond stretch vibration by infrared spectra,²⁷ which indicates the formation of only one Si-C bond per alkyne molecule. The reason for these differences in the reactivity of 1-alkynes is unclear. Sieval *et al.* postulated that the second Si-C bond has to be formed to the next-nearest Si surface atom on the H-terminated Si(111) surface,³⁵ which would give rise to a five-membered ring structure, in which considerable deformation of the Si-C bonds is required. This can prohibit the formation of two Si-C bonds per molecule on this surface.

In this section, we will discuss the other possible structures of alkyne-derived monolayers on Si(111) surfaces using the molecular mechanics method. Scheme 2 shows the possible formation of two Si-C bonds per molecule (*i.e.*, b and c in Scheme 2). Perhaps theoretical calculations can provide further insight into the way that 1-alkynes are bound to the Si(111) surface. Considering the discussion above, an (8 × 8) simulation cell containing 32 organic molecules was designed. For the octyne reacting with an H-terminated Si(111) surface, three possible structures can be designed according to Sieval's work on the Si(100) surface, having:³⁵ one Si-C bond (a in Scheme 2), two Si-C bonds of a 1,2-bridge (b in Scheme 2) or two Si-C bonds of a 1,1-bridge (c in Scheme 2). In the molecular mechanic calculations, the best substitution percentage of 50% was selected, as above. The relative energy per molecule calculated using eqn. (1) is given in Table 4.

As seen from Table 4, the energy per molecule with one Si-C bond is the lowest, and the higher energies are found in the 1,1-bridge and 1,2-bridge structures. At the same time, a similar conclusion is reached as concerns the three possible structures of phenylacetylene reacting with an H-terminated Si(111) surface; the energy with one Si-C bond is also the lowest. This means that formation of one Si-C bond leads to the stablest structure. These results can be used to explain why the C=C bond is always found when an alkyne reacts with the H-terminated Si(111) surface under thermal or photochemical reaction conditions, that is, the alkyne C≡C can only react once with the H-terminated Si(111) surface. In Cicero's work,²⁷ the C=C bond stretch vibration was observed. This means that the possible structures b and c in Scheme 2 do not exist in their experiments, which is also supported by our calculated energy results. Like Sieval's interpretation above,³⁵ the double reaction of the C≡C bond is difficult when the Si(111) surface only contains Si-H groups. H atoms may be essential to the reaction of alkyne with the Si surface.

3.7 The structure of different derived monolayers on a Si surface

Cicero *et al.* made different monolayers using photoreaction, such as octene- or octyne-derived monolayers and styrene- or phenylacetylene-derived monolayers.²⁷ Some properties were determined from the FTIR and XPS spectra. In the reaction of the alkyne C≡C bond with the H-terminated Si surface, structures containing two Si-C bonds per molecule (*i.e.*, 1,1-bridge and 1,2-bridge) are not formed, according to the discussion above. Thus, only alkyl monolayers containing a C=C bond in the molecule are discussed in the investigation of structures on the Si(111) surface. Other monolayers besides the octene-derived monolayer are discussed in the following. The geometry of the octyne-derived monolayer (Fig. 7) takes on an unordered structure in contrast to the octene-derived monolayer (see Fig. 6) when a substitution percentage of 50% and substitution pattern i (in Fig. 3) are selected. This means that the substitution percentage of the octene-derived monolayer

Table 4 Relative energies of the alkyne-derived monolayer structures a, b and c in Scheme 2 as obtained from molecular mechanics

Structure	Octyne-derived	Phenylacetylene-derived
One C-Si bond	-16.451	-13.694
1,2-Bridging, two C-Si bonds	+53.727	+72.333
1,1-Bridging, two C-Si bonds	+114.638	+146.308

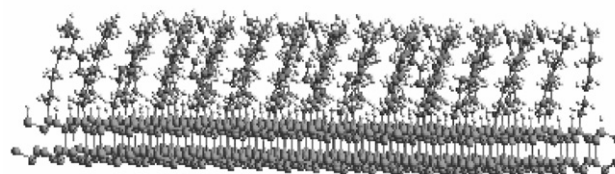


Fig. 7 The octyne-derived monolayer on the Si(111) surface after optimization.

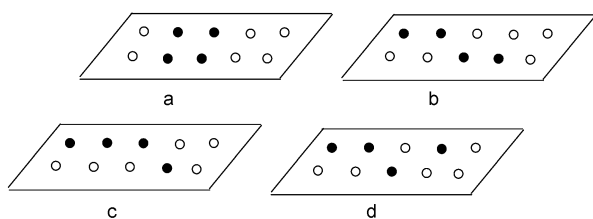


Fig. 8 Simulation cells of different substitution patterns at 40% substitution for octene- or octyne-derived monolayers.

should be larger than that of the octyne-derived monolayer, despite its having the substitution percentage of 50%. But the tilt angle of around 10° does not change. The unordered structure of the octyne-derived monolayer at 50% substitution shows that the double bond of the alkyl chain is an important factor affecting of the structure of alkyl chains on Si(111) surfaces.

For the styrene- or phenylacetylene-derived monolayers, it is difficult to design a 40% substitution pattern in a small unit cell. When different (2×5) unit cells were designed, several tens of substitution patterns were used to find the best structures. Fig. 8 shows four substitution patterns with the highest or relatively low energies. The calculated results show that substitution patterns with the lowest or highest energies for the alkyl chain are the same for octene-, octyne-, styrene- and phenylacetylene-derived monolayers. For these substitution patterns, we see that substitution pattern a has the highest energy and b has a relatively low energy. This conclusion proves our discussion above, that two or three neighboring alkyl chains are favorable for formation of the alkyl monolayer on the surface. Thus, the conclusion that substitution pattern i in Fig. 4 is the stablest geometry is valid not only for octene- or octyne-derived monolayers but also for styrene- or phenylacetylene-derived monolayers (pattern b in Fig. 8). Furthermore, some structural properties of the alkyl monolayer can also be obtained. The tilt angle of the styrene- or phenylacetylene-derived monolayer is around 9° , and the substitution percentage is perhaps slightly larger than 40%.

From our molecular mechanics calculations, the bond angle of Si–C–C in the octene-derived monolayer is equal to 119.0° , which is bigger than the 109.5° in Zhang's *ab initio* study.²⁶ This difference is because Zhang's model system is too small to represent real alkyl monolayers on a Si(111) surface, and his calculation could produce big errors in contrast to a big system containing boundary conditions. For a single alkyl chain system, the C and Si atoms in the Si–C–C system may compose a tetrahedron, so the bond angle of Si–C–C should be equal to 109.5° .²⁶ But for a big system, for example, in an (8×8) simulation cell, each alkyl chain on the Si(111) surface would experience steric effects from the other chains around it, which would affect the structure of Si and C atoms on Si(111) surface, meaning that an ideal tetrahedron geometry of Si and C atoms would not be formed. Thus, the bond angle of Si–C–C in a big simulation system should be different from that in a small tetrahedral system.

Other bond angles and dihedral angles of organic monolayers are listed in Table 5. The values show that the bond angles of octene- (or styrene-)derived monolayers are smaller than those of octyne- (or phenylacetylene-)derived monolayers. This indicates that the double bond in the organic chain can affect the steric structure. In the other words, the double bond of Si–C=C–C is the main reason that the properties of two organic monolayers on Si(111) surface are different. In addition, steric effects are important in determining the structure of the monolayer.

Table 5 The bond and dihedral angles of the organic monolayer

Adsorbate	$\angle \text{Si-C-C}^a / ^\circ$	$\angle \text{Si-C-C-C}^a / ^\circ$
Octene	119.0	160.8
Octyne	124.7	161.4
Styrene	123.6	171.3
Phenylacetylene	125.6	176.0

^a Errors in bond and dihedral angles are $\pm 0.5^\circ$.

4. Conclusion

In the present work molecular mechanics simulations have been performed to study the substitution percentage and the substitution pattern of eight-carbon organic monolayers. The basic conclusions drawn are as follows. (1) The substitution percentage for octene- or octyne-derived monolayers on Si(111) surface is equal to 50%, and 40% for styrene or phenylacetylene-derived monolayers. These results are in good agreement with the experimental results. (2) The stablest structures of organic monolayers on a Si(111) surface obtained from alkynes and alkenes have the same substitution pattern. (3) The free radial theory shows that the steric effect of alkyl chains on Si(111) surfaces is important in the formation of the organic monolayer, besides van der Waals interaction between different alkyl chains. (4) The (8×8) or (8×16) simulation cells with boundary conditions can represent the microstructural properties of the monolayer at the molecular level. The densely packed, well-ordered monolayer can be modelled by the (8×16) simulated cell. (5) To investigate the structural properties of the big system containing boundary conditions, molecular mechanics methods can give some results that can also be obtained *via ab initio* calculations. Thus, molecular simulations may be considered as a useful adjunct to experiments.

Acknowledgements

The authors thank Prof. Xinsheng Zhao (Beijing University, China) for useful discussions. This work was supported by the National Natural Science Foundation of China (No. 20173032).

References

- M. R. Linford, P. Fenter, P. M. Eisenberger and C. E. D. Chidsey, *J. Am. Chem. Soc.*, 1995, **117**, 3145.
- A. B. Sieval, A. L. Demirel, J. W. M. Nissink, M. R. Linford, J. H. van der Maas, W. H. de Jeu, H. Zuihof and E. J. R. Sudhölter, *Langmuir*, 1998, **14**, 1759.
- G. J. Batinica and J. E. Crowell, *J. Phys. Chem. B*, 1998, **102**, 4135.
- A. Juang, O. A. Scherman, R. H. Grubbs and N. S. Lewis, *Langmuir*, 2001, **17**, 1321.
- A. Bansal, X. Li, I. Lauermann, N. S. Lewis, S. I. Yi and W. H. Weinberg, *J. Am. Chem. Soc.*, 1996, **118**, 7225.
- A. Bansal and N. S. Lewis, *J. Phys. Chem. B*, 1998, **102**, 4058.
- A. Bansal and N. S. Lewis, *J. Phys. Chem. B*, 1998, **102**, 1067.
- R. Boukherroub, S. Morin, F. Bensebaa and D. D. M. Wayner, *Langmuir*, 1999, **15**, 3831.
- F. Effenberger, G. Götz, B. Bidlingmaier and M. Wezstein, *Angew. Chem., Int. Ed.*, 1998, **37**, 2462.
- C. Henry De Villeneuve, J. Pinson, M. C. Bernard and P. Allongue, *J. Phys. Chem. B*, 1997, **101**, 2415.
- M. Mitsuya, *Langmuir*, 1994, **10**, 1635.
- M. Mitsuya, *Appl. Phys. Lett.*, 1997, **70**, 961.
- M. Mitsuya and N. Sugita, *Langmuir*, 1997, **13**, 7075.
- M. Mitsuya and N. Sato, *Langmuir*, 1999, **15**, 2099.
- X. Cao and R. J. Hamers, *J. Am. Chem. Soc.*, 2001, **123**, 10988.
- R. Boukherroub and D. D. M. Wayner, *J. Am. Chem. Soc.*, 1999, **121**, 11513.

- 17 H. Z. Yu, S. Morin and D. D. M. Wayner, *J. Phys. Chem. B*, 2000, **104**, 11 157.
- 18 A. Bansal, X. Li, S. I. Yi, W. H. Weinberg and N. S. Lewis, *J. Phys. Chem. B*, 2001, **105**, 10 266.
- 19 D. Gorelik and G. Haase, *J. Phys. Chem. B*, 2000, **104**, 2575.
- 20 M. A. Rezaei, B. C. Stipe and W. Ho, *J. Phys. Chem. B*, 1998, **102**, 10 941.
- 21 T. Homma, C. P. Wade and C. E. D. Chidsey, *J. Phys. Chem. B*, 1998, **102**, 7919.
- 22 U. Birkenheuer, U. Gutdeutsch and N. Rösch, *Surf. Sci.*, 1998, **409**, 213.
- 23 S. Gokhale, P. Trischberger, D. Menzel, W. Widdra, H. Dröge, H. P. Steinrück, U. Birkenheuer, U. Gutdeutsch and N. Rösch, *J. Chem. Phys.*, 1998, **108**, 5554.
- 24 C. W. Bauschlicher and M. Rosi, *Theor. Chem. Acc.*, 1997, **97**, 213; C. W. Bauschlicher and M. Rosi, *J. Phys. Chem. B*, 1998, **102**, 2403.
- 25 A. B. Sieval, B. van den Hout, H. Zuihof and E. J. R. Sudhölter, *Langmuir*, 2000, **16**, 2987; A. B. Sieval, B. van den Hout, H. Zuihof and E. J. R. Sudhölter, *Langmuir*, 2001, **17**, 2172.
- 26 L. Zhang, K. Wesley and S. Jiang, *Langmuir*, 2001, **17**, 6275.
- 27 R. L. Cicero, M. R. Linford and C. E. D. Chidsey, *Langmuir*, 2000, **16**, 5688.
- 28 A. K. Rappé, C. J. Casewit, K. S. Colwell, W. A. Goddard and W. M. Skiff, *J. Am. Chem. Soc.*, 1992, **114**, 10 024.
- 29 H. Sun, P. Ren and J. R. Fried, *Comput. Theor. Polym. Sci.*, 1998, **8**, 299.
- 30 H. Sun, *J. Phys. Chem.*, 1998, **102**, 7338.
- 31 J. Terry, M. R. Linford, C. Wigren, R. Cao, P. Planetta and C. E. D. Chidsey, *Appl. Phys. Lett.*, 1997, **71**, 1056.
- 32 J. M. Buriak and M. J. Allen, *J. Am. Chem. Soc.*, 1998, **120**, 1339.
- 33 J. M. Buriak, M. P. Stewart, T. W. Geders, M. J. Allen, H. C. Choi, J. Simth, D. Raftery and L. T. Canham, *J. Am. Chem. Soc.*, 1999, **121**, 11 491.
- 34 J. E. Bateman, R. D. Eagling, D. R. Worrall, B. R. Horrocks and A. Houlton, *Angew. Chem., Int. Ed.*, 1998, **37**, 2683.
- 35 A. B. Sieval, R. Opitz, H. P. A. Maas, M. G. Schoeman, G. Meijer, F. J. Vergeldt, H. Zuilhof and E. J. R. Sudhölter, *Langmuir*, 2000, **16**, 10 359.